

Air Entrainment in the Developing Flow Region of Plunging Jets—Part 1: Theoretical Development

P. D. Cummings

Maritime Engineer,
Kinhill Engineers,
299 Coronation Drive,
Brisbane QLD 4064,
Australia

H. Chanson

Senior Lecturer,
Fluid Mechanics,
Hydraulics and Environmental Engineering,
Department of Civil Engineering,
The University of Queensland,
Brisbane QLD 4072,
Australia

Air-water bubbly flows are encountered in many engineering applications. One type of air-water shear flows is the developing flow region of a plunging jet. The mechanisms of air entrainment by plunging liquid jets are discussed in the light of new experimental evidence. Then the air bubble diffusion is analyzed analytically in the near-flow field of both circular and two-dimensional plunging jets. The theoretical developments are compared with existing circular plunging jet data and new experiments performed with a two-dimensional vertical supported jet. The study highlights two mechanisms of air entrainment at the plunge point depending upon the jet impact velocity and results suggest that the dispersion of air bubbles within the shear layer is primarily an advective diffusion process.

Introduction

When a water jet impinges a pool of water at rest, air bubbles may be entrained and carried away below the pool free surface (Figs. 1 and 2). This process is called plunging jet entrainment.

In chemical engineering, plunging jets are used to stir chemical as well as to increase gas-liquid transfer (e.g., McKeogh and Irvine, 1981, Bin, 1993). In sewage and water treatment plants, aeration cascades combine the effects of flow aeration and high turbulence level, enhancing the mass transfer of volatile gases (e.g., oxygen, nitrogen, volatile organic compounds). Plunging jet devices are used also in industrial processes (e.g., bubble flotation of minerals). Planar plunging jets are observed at weir spillways and overfalls. Some similarity between the planar plunging jet and the jet of a plunging breaking wave in the ocean was noted by several authors (e.g., Coles, 1967, Longuet-Higgins, 1982). A related case is the continuous impingement of a solid surface into a liquid pool and the associated air entrainment (e.g., Burley and Jolly, 1984). Despite the wide range of applications, few studies investigated air bubble entrainment in the developing shear layer of plunging jets.

At a plunging jet, the near-flow field (below the impingement point) is characterised a developing shear layer with some momentum transfer between the high-velocity jet core and the receiving pool of water, at rest at infinity (Fig. 1). In presence of air entrainment, an air bubble diffusion layer takes places (Figs. 1 and 2). The air diffusion layer may not coincide with the momentum shear layer. Further downstream the jet flow becomes fully-developed.

In the present paper and its companion (Cummings and Chanson, 1997), the authors investigate the air bubble entrainment in the developing region of plunging jet flows. New experiments were performed with a vertical supported jet (Fig. 2, Table 1). The results provide new information on the air entrainment mechanisms, the advective diffusion of air bubbles, the momentum exchange process, and the distributions of chord lengths of entrained bubbles. The mechanisms of air entrainment and air bubble diffusion are discussed in this paper. The experimental apparatus, velocity distributions and the chord length data are

described in the companion paper. It is the purpose of these two papers to assess critically the overall state of this field, to present new analysis and experimental results, to compare these with existing data, and to present new compelling conclusions regarding momentum and air concentration development of jet-entrained gas-liquid flows. These conclusions will bring together the behavior of both axisymmetric and planar jets impinging on free surfaces.

Background

Several researchers (see bibliographic review by Bin, 1993) showed interest in circular plunging jets. Numerous experiments were performed with small circular jets (typically $\phi_1 < 5$ mm). Most researchers investigated qualitatively the air entrainment process.

Several studies showed that air entrainment takes place when the jet impact velocity exceeds a characteristic velocity. And the jet length and jet turbulence level both affect the quantitative value of that characteristic velocity (see next section). The mechanisms of air entrainment depends upon the jet velocity at impact, the physical properties of fluid, the jet nozzle design, the length of free-falling jet and the jet turbulence (Bin, 1993).

Some studies, in particular the thesis of Van de Sande (1974), McKeogh (1978), Van de Donk (1981), and Evans (1990), contributed significantly to our present understanding of the entrainment/entrapment process of air at the impingement point. Unlikely only a small number of studies investigated the flow field below the impingement point: e.g., McKeogh and Irvine (1981), Van de Donk (1981) and Bonetto and Lahey (1993). McKeogh and Irvine (1981) and Van de Donk (1981) recorded air concentration profiles and velocity distributions primarily in the fully-developed flow region, while Bonetto and Lahey (1993) presented results obtained in both the developing and fully-developed flow regions.

Two-dimensional plunging jet flows received much less attention. Some studies (Goldring et al., 1980, Sene, 1988) were performed with supported jets to investigate the flow patterns but no information is available on the distributions of air content and velocity below the impingement point.

Bin (1993) highlighted the lack of information on the velocity profiles and air content distributions in the vicinity of the impingement point and in the near-flow field.

Contributed by the Fluids Engineering Division for publication in the JOURNAL OF FLUIDS ENGINEERING. Manuscript received by the Fluids Engineering Division December 5, 1995; revised manuscript received April 1, 1997. Associate Technical Editor: O. C. Jones.

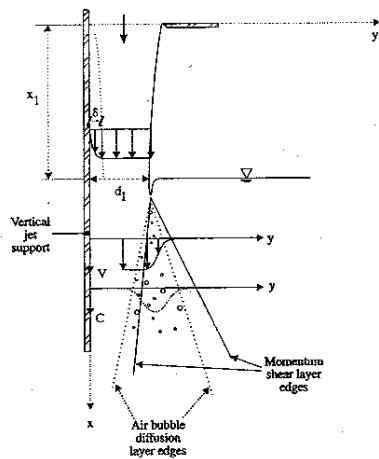


Fig. 1 Sketch of air entrainment at a vertical supported jet, a circular plunging jet and a free-falling two-dimensional plunging jet

Mechanisms of Air Bubble Entrainment

In a plunging jet situation, air bubbles start to be entrained when the jet impact velocity V_1 exceeds a critical value. Dimensional analysis suggests that this critical velocity is a function of the fluid properties, the turbulence characteristics (velocity



Fig. 2 Photograph of air bubble entrainment at a vertical supported jet (side view). The support is on the left. The air bubble diffusion layer is clearly seen with the white downward diffusion cone. On the right note the rising air bubbles. $V_1 = 6.14$ m/s.

and length scales) and the angle of the jet with the free-surface. For the vertical supported jet experiment, the authors observed air bubble entrainment for $V_1 > 1.1$ to 2.0 m/s when the jet turbulence intensity at impact Tu varies from 1.3 down to 0.3 percent. With vertical circular plunging jets, McKeogh (1978) and Ervine et al. (1980) observed air entrainment for $V_1 > 0.8$ m/s when the turbulence intensity at the jet nozzle was larger than 3 percent, and they noticed larger inception velocities at lower turbulence levels at nozzle.

When air bubbles are entrained, visual and photographic observations obtained during the present series of experiments indicate two major air entrainment processes. For low velocities (i.e., $V_1 < 2$ m/s), air bubble entrainment was observed to be caused by the pool of water being unable to follow the undulations of the jet surface and small air pockets are formed. Air enters the flow following the passage of these disturbances through the interface between the jet and the receiving fluid (Fig. 3(a)). High-speed videocamera images indicates that most bubbles are entrained as individual bubbles and air pockets, which are subsequently broken up into smaller size bubbles.

For large jet impact velocities (i.e., $V_1 > 3$ to 8 m/s), experiments on both circular (Van de Sande and Smith 1973) and

Nomenclature

C = air concentration defined as the volume of air per unit volume of air and water; it is also called void fraction	q_{air} = air discharge per unit width (m^2/s)	x_1 = distance (m) between the channel intake and the impact flow conditions
D_t = turbulent diffusivity (m^2/s)	q_w = water discharge per unit width (m^2/s)	Y = characteristic flow depth or flow thickness (m) normal to the flow direction
D^* = dimensionless turbulent diffusivity: $D^* = D_t/(VY)$; $D^* = D_t/(V_1 d_1)$ for two-dimensional shear flow and $D^* = D_t/(V_1 r_1)$ for circular jet	r = radial distance (m) from the jet centerline	y = distance (m) measured normal to the flow direction
d = flow depth or jet thickness (m) measured perpendicular to the flow direction	r' = radial coordinate (m)	δ = boundary layer thickness (m) defined in term of 99% of the maximum velocity
d_1 = jet thickness (m) at the impact with the receiving pool of liquid	r_1 = jet radius (m) at impact	δ_{air} = thickness (m) of the air sheet set into motion by a high-velocity plunging jet (Fig. 3)
g = gravity constant: $g = 9.80$ m/s ² in Brisbane, Australia	Tu = turbulence intensity defined as: $Tu = u'/V$	θ, θ' = radial angular coordinate
I_0 = modified Bessel function of the first kind of order zero	Tu_0 = turbulence intensity measured at jet nozzle	\varnothing = diameter (m)
Q_{air} = air discharge (m^3/s)	u = dimensionless variable	
Q_w = water discharge (m^3/s)	u' = root mean square of longitudinal component of turbulent velocity (m/s)	
	V = velocity (m/s)	
	V_1 = mean flow velocity (m/s) at jet impact	
	W = channel width (m)	
	x = distance along the flow direction (m)	
		Subscript
		air = air flow
		w = water flow
		1 = impact flow conditions

Table 1 Experimental flow conditions of vertical plunging jets

Ref. (1)	Run (2)	q_w m^2/s (3)	V_j m/s (4)	$x_1^{(a)}$ m (5)	Comments (6)
McKeogh and Ervine (1981)			3.13 3.9 2.5 3.3		Circular jet. Fig. 6. $\varnothing_1 = 0.009$ m. $Tu_0 = 5\%$. Fig. 8 and 9. $\varnothing_1 = 0.009$ m. $Tu_0 = 1\%$. Fig. 9. $\varnothing_1 = 0.009$ m. $Tu_0 = 1\%$. Fig. 9. $\varnothing_1 = 0.009$ m. $Tu_0 = 1\%$.
Van de Donk (1981)	VDD1 VDD2		4.463 10.19	0.20 0.20	Circular jet. Fig. 3.22. $\varnothing_1 = 0.0057$ m. Fig. 3.23. $\varnothing_1 = 0.0059$ m.
Bonetto and Lahey (1993)	B11 B13 B16		6.18 8.91 5.27	0.03 0.03 0.01	Circular jet. Fig. 11. $\varnothing_1 = 0.0051$ m. Fig. 13. $\varnothing_1 = 0.0051$ m. Fig. 16. $\varnothing_1 = 0.0051$ m.
Chanson (1995a)	F1 F2 F3 F4 F5	0.024 0.048 0.072 0.096 0.108	2.36 4.06 5.89 8.0 9.0	0.090 0.090 0.090 0.090 0.090	Two-dimensional supported jet. $W = 0.269$ m. $d_i = 0.0102$ m. $Tu = 1.70\%$. $d_i = 0.0118$ m. $Tu = 1.50\%$. $d_i = 0.0122$ m. $Tu = 0.74\%$. $d_i = 0.012$ m. $d_i = 0.012$ m.
Present study	2-m/s 6-m/s	0.0240 0.0720	2.39 6.14	0.0875 0.0875	Two-dimensional supported jet. $W = 0.269$ m. $d_i = 0.010$ m. $Tu = 1.6\%$. $d_i = 0.0117$ m. $Tu = 0.75\%$.

Notes:

(a): Longitudinal distance between the nozzle and the free-surface pool.

Tu: Jet turbulence intensity at impact.

Tu₀: Turbulent intensity measured at jet nozzle.

planar (authors' experiments) plunging jets indicate a qualitative change in the air entrainment process. A thin sheet of air, set into motion by shear forces at the surface of the jet, enters the flow at the impact point (Fig. 3(b)). The air sheet behaves as a ventilated cavity (e.g., Michel, 1984): the length of the air layer fluctuates considerably and air pockets are entrained by discontinuous "gusts" at the lower end of the air layer (Fig. 3). The elongated air sheet is intermittently broken by a "re-entrant jet" mechanism. Visual observations and conductivity probe measurements show clearly that some air is entrained in the form of elongated pockets. For jet velocities between 3 and 6 m/s, the authors observed air sheet thickness δ_{al} of about 0.5

to 5 mm. The jet velocity at which the air layer appears is an inverse function of jet turbulence: i.e., for 'smooth' jets, the air sheet will appear at larger velocities than for 'rough' jets.

The observations of air sheet thickness can be compared with the analysis of Lezzi and Prosperetti (1991) and Bonetto et al. (1994) (Table 2). The former suggested that the instability responsible for air entrainment is caused by gas viscosity while the latter study assumed that gas entrainment is induced by a Helmholtz-Taylor instability. The analysis of Bonetto et al. (1994) seems to fit better the authors' observations (Table 2). But additional data are required to confirm this point.

Analysis of the Air Bubble Diffusion Process

The air bubble diffusion at a plunging liquid jet is a form of advective diffusion. For a small control volume, the continuity equation for air in the air-water flow is:

$$\text{div}(C\vec{V}) = \text{div}(D_i \text{grad } C) \tag{1}$$

where D_i is the turbulent diffusivity. Equation (1) implies a constant air density (i.e. neglecting compressibility effects), it neglects buoyancy effects and is valid for a steady flow situation.

Considering a *circular plunging jet*, assuming a uniform velocity distribution, for a constant diffusivity (in the radial direction) independent of the longitudinal location and for a small control volume delimited by streamlines (i.e., stream tube), Eq. (1) becomes a simple diffusion equation:

$$\frac{V_j}{D_i} \frac{\partial C}{\partial x} = \frac{1}{r} \frac{\partial}{\partial r} \left(r \frac{\partial C}{\partial r} \right) \tag{2}$$

where x is the longitudinal direction, r is the radial direction, and the diffusivity term D_i averages the effects of the turbulent diffusion and of the longitudinal velocity gradient. The boundary conditions of the axisymmetric problem are: $C(x < x_1, r) = 0$ and a circular source of total strength Q_{air} at $\{x - x_1 = 0, r = r_1\}$.

The problem can be solved analytically by applying a superposition method. At each position $\{x, r, \theta'\}$, the diffusion

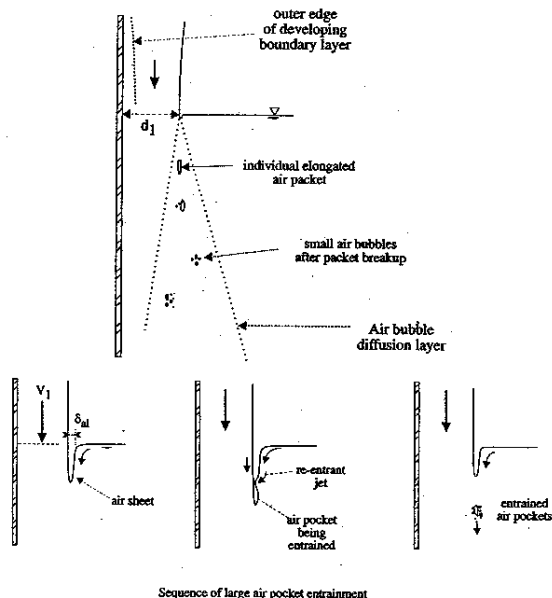


Fig. 3 Sketch of air entrainment at a vertical supported jet. (a) Low-velocity air entrainment mechanism; (b) high-velocity air entrainment process

Table 2 Thickness of air sheet set into motion in high-velocity two-dimensional plunging jet

Reference (1)	δ_{ai}				Comments (7)
	$V_1 = 2.4$ m/s (2)	$V_1 = 3$ m/s (3)	$V_1 = 6$ m/s (4)	$V_1 = 9$ m/s (5)	
Experimental data					
Present data	N/A		0.5 to 5 mm		Two-dimensional jet.
Analysis (*)					
Lezzi and Prosperetti (1991)	0.065 mm	0.06 mm	0.04 mm	0.03 mm	Calculations deduced from the measured air entrainment flux.
Bonetto et al. (1994)	0.65 mm	N/A	N/A	6.6 mm	

Note:

(*) Calculations applied to two-dimensional plunging jet.

equation is solved for each point source of strength δq_{air} located at $\{0, r_1, \theta'_1\}$. The contribution of each point source is:

$$\delta C = \frac{\delta q_{air} r_1 \delta \theta'_1}{4\pi D_i (x - x_1)} \exp\left(-\frac{V_1}{4D_i(x - x_1)} r'^2\right) \quad (3)$$

where $r'^2 = (r \cos \theta' - r_1 \cos \theta'_1)^2 + (r \sin \theta' - r_1 \sin \theta'_1)^2$, and $\{r, \theta'\}$ and $\{r_1, \theta'_1\}$ are the polar coordinates of the current point and of the point source respectively. The general solution of the air bubble diffusion equation is solved by superposing all the point sources:

$$C = \int_0^{2\pi} \delta C d\theta'_1 \quad (4)$$

and using the definition of the air flow rate:

$$Q_{air} = 2\pi r_1 \delta q_{air} \quad (5)$$

The solution of the air bubble diffusion becomes:

$$C = \frac{Q_{air}}{Q_w} \frac{1}{4D^* \frac{x - x_1}{r_1}} \exp\left(-\frac{1}{4D^*} \frac{\left(\frac{r}{r_1}\right)^2 + 1}{\frac{x - x_1}{r_1}}\right) \times I_0\left(\frac{1}{2D^*} \frac{\frac{r}{r_1}}{\frac{x - x_1}{r_1}}\right) \quad \text{Circular plunging jet} \quad (6)$$

where I_0 is the modified Bessel function of the first kind of order zero¹ and $D^* = D_i/(V_1 r_1)$.

Considering a *two-dimensional free-falling jet*, the air bubbles are supplied by point sources located at $\{x = x_1, y = +d_1/2\}$ and $\{x = x_1, y = -d_1/2\}$ in the two-dimensional plane. Assuming a uniform velocity distribution, for a diffusion coefficient independent of the transverse location and for small control volume $\{dx, dy\}$ limited between two streamlines, the continuity equation (Eq. (1)) becomes a simple diffusion equation:

$$\frac{V_1}{D_i} \frac{\partial C}{\partial x} = \frac{\partial^2 C}{\partial y^2} \quad (7)$$

where y is the distance normal to the jet centerline or jet support (Fig. 1). The boundary conditions of the two-dimensional free-jet flow are: $C(x < x_1, y) = 0$ and two point sources of equal strength $\{0.5Q_{air}/W\}$ located at $\{x_1, +d_1/2\}$ and $\{x_1, -d_1/2\}$.

¹ $I_0(u) = 1 + (u^2/2^2) + (u^4/2^2*4^2) + (u^6/2^2*4^2*6^2) + \dots$

The problem can be solved by superposing the contribution of each point source. The solution of the diffusion equation is:

$$C = \frac{1}{2} \frac{Q_{air}}{Q_w} \frac{1}{\sqrt{4\pi D^* \frac{x - x_1}{d_1}}} \left(\exp\left(-\frac{1}{4D^*} \frac{\left(\frac{y - 1}{d_1}\right)^2}{\frac{x - x_1}{d_1}}\right) + \exp\left(-\frac{1}{4D^*} \frac{\left(\frac{y + 1}{d_1}\right)^2}{\frac{x - x_1}{d_1}}\right) \right)$$

two-dimensional free-falling plunging jet (8a)

where Q_{air} is the volume air flow rate and d_1 is the thickness of the free-jet at impact. D^* is a dimensionless diffusivity: $D^* = D_i/(V_1 d_1)$.

Considering a *two-dimensional supported jet*, the air bubbles are supplied by a point source located at $\{x = x_1, y = +d_1\}$ in the two-dimensional plane and the strength of the source is Q_{air}/W . The diffusion equation can be solved by applying the method of images and assuming an infinitesimally long support. It yields:

$$C = \frac{Q_{air}}{Q_w} \frac{1}{\sqrt{4\pi D^* \frac{x - x_1}{d_1}}} \left(\exp\left(-\frac{1}{4D^*} \frac{\left(\frac{y - 1}{d_1}\right)^2}{\frac{x - x_1}{d_1}}\right) + \exp\left(-\frac{1}{4D^*} \frac{\left(\frac{y + 1}{d_1}\right)^2}{\frac{x - x_1}{d_1}}\right) \right)$$

two-dimensional supported plunging jet (8b)

where Q_{air} is the volume air flow rate, D^* is a dimensionless diffusivity: $D^* = D_i/(V_1 d_1)$. Note that d_1 is the thickness of the supported jet at impact.

Remarks. Equations (6), (8a), and (8b) are new analytical solutions of the advective diffusion of air bubbles (Eq. (1)). The two-dimensional and axisymmetrical solutions differ however because of the boundary conditions and of the integration method.

Note first that Eqs. (6), (8a), and (8b) are three-dimensional solutions of the diffusion equation. They are valid in both the developing bubbly region and in the fully-aerated flow region. For circular plunging jet and two-dimensional free jets, the core

of the jet (i.e., $r = 0$, $y = 0$) becomes aerated, respectively, for:

$$\frac{D_i(x - x_1)}{V_i r_i^2} > 0.039$$

fully-aerated jet flow region [$C(r = 0) > 0.01$] (9a)

$$\frac{Q_{air}}{Q_w} \frac{\exp\left(-\frac{1}{4D^*} \frac{1}{x - x_1} \frac{1}{d_1}\right)}{\sqrt{4\pi D^* \frac{x - x_1}{d_1}}} > 0.01$$

fully-aerated jet flow region [$C(y = 0) > 0.01$] (9b)

Note also that the solutions of two-dimensional plunging jet flows (Eq. (8a) and (8b)) derive from a classical solution of the two-dimensional advective diffusion equation (e.g., Crank, 1956, Fischer et al., 1979). In the developing air bubble diffusion layers (i.e., $C(y = 0) = 0$), Eqs. (8a) and (8b) can be approximated, respectively, by:

$$C = \frac{1}{2} \frac{Q_{air}}{Q_w} \frac{1}{\sqrt{4\pi D^* \frac{x - x_1}{d_1}}} \exp\left(-\frac{1}{4D^*} \frac{\left(\frac{y - 1}{d_1} - 1\right)^2}{\frac{x - x_1}{d_1}}\right)$$

free jet (10a)

$$C = \frac{Q_{air}}{Q_w} \frac{1}{\sqrt{4\pi D^* \frac{x - x_1}{d_1}}} \exp\left(-\frac{1}{4D^*} \frac{\left(\frac{y - 1}{d_1}\right)^2}{\frac{x - x_1}{d_1}}\right)$$

supported jet (10b)

Note further that the analytical developments imply a constant diffusion coefficient D_i , where D_i averages the effects of turbulent dispersion and streamwise velocity gradient. Such an assumption does not reflect the real nature of the turbulent shear layer nor the existence of vortical structures (e.g., Fig. 4(a), Chanson, 1995b). Nevertheless, the agreement between experiments and theory is within the accuracy of the instrumentation, suggesting that the air bubble diffusion process is little affected by the turbulent shear flow.

Additional details of the calculations were presented in Chanson (1995a).

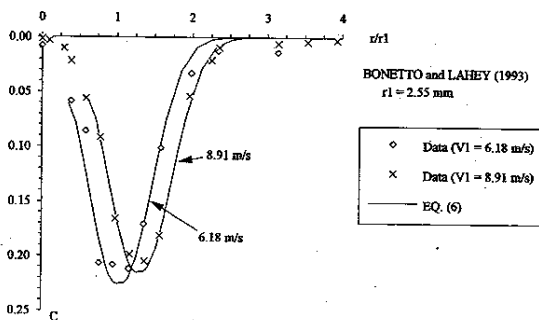


Fig. 4 Air bubble diffusion in the developing shear region of circular jet. Comparison between Eq. (6) and experimental data (Bonetto and Lahey, 1993).

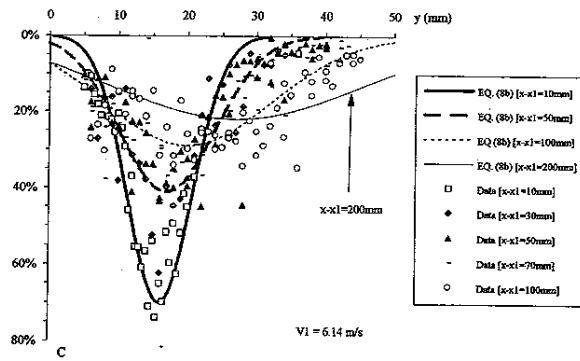


Fig. 5 Distributions of air concentration in the developing flow region of vertical supported plunging jets. Comparison between Eq. (8b) and experimental data (present study; impact velocity $V_1 = 6.14$ m/s).

Results and Discussion

Comparison With Experimental Data. Equations (6) and (8b) have been compared successfully with experimental data (Van de Donk, 1981; Bonetto and Lahey, 1993; Chanson 1995a, Present study). Details of the experimental flow conditions are listed in Table 1. Figures 4 and 5 show some examples.

Figure 4 compares Eq. (6) with the recent data of Bonetto and Lahey (1993) while Chanson's (1995a) data are compared with Eq. (8b). Both Figs. 4 and 5 show a good agreement between experimental data and analytical solutions of the advective diffusion equation.

Note that Eq. (8a) cannot be verified in the fully-aerated flow region (i.e., $C(y = 0) > 0$) because of the absence of experimental data.

Discussion. Downstream of the entrainment point, the distributions of air content exhibit a distinctive shape (Figs. 4 and 5) which can be modelled by an advective diffusion equation. The analytical integration of Eq. (1) provides three-dimensional solutions (Eqs. (6), (8a), (8b)) which are valid in both the developing bubbly region and in the fully-aerated flow region.

Three parameters characterise the advective diffusion solutions (Eqs. (6) and (8)): the air flow rate Q_{air}/Q_w , the dimensionless diffusivity D^* and eventually the location of the symmetry line of the air content profile. For the experiments of Van de Donk (1981), Chanson (1995a) and the authors, the data and analytical solutions were best fitted with the air flow rate and the diffusivity being constants independent of the longitudinal position ($x - x_1$). For the authors' experiments, the air flow rate was calculated from the continuity equation for air as $q_{air} = \int_0^\infty CV dy$ where C and V are local values (Cummings and Chanson 1997). Such results and the close agreement between data and analytical solutions suggest that the diffusion of air bubbles below the impingement point is primarily an advective diffusion process.

Note that the data of Bonetto and Lahey (1993) could not be checked in details because of the insufficient number of data.

The authors wish to emphasize that Eqs. (6) and (8) are not valid very-close to the entrainment point. At the impingement point, the air entrainment/entrapment process cannot be simply modelled by an advective diffusion mechanism. For the authors' experiments, Eq. (8) and experimental data were in good agreement for $(x - x_1) \geq 20$ mm.

Conclusion

The authors have investigated the mechanisms of air entrainment at plunging liquid jets. They performed new measurements in a large vertical supported jet experiment ($0.3 < V_1 < 9$ m/

s). The flow field below the impingement point was investigated with conductivity probes and high-speed pictures.

1 Air bubble entrainment is observed when the jet impact velocity becomes larger than a critical value of about 1.1 to 2.0 m/s for the two-dimensional vertical jet experiment.

2 At the plunge point, two mechanisms of air entrainment can be observed: individual bubble entrainment at low-jet velocity (i.e. $V_1 < 2$ m/s), and a ventilated-cavity mechanism at high-velocities (i.e., $V_1 > 3$ to 8 m/s).

3 Below the impingement point, the air concentration profiles follow closely new analytical solutions of the diffusion equation for both circular plunging jets (Eq. (6)) and two-dimensional plunging jets (Eq. (8)). The close agreement between data and theory suggests that the dispersion of air bubbles within the shear layer is primarily an advective diffusion process.

In a companion paper (Cummings and Chanson, 1997), the velocity field will be described and bubble chord length distributions will be presented.

Acknowledgments

The authors want to thank particularly Professor C. J. Apelt, University of Queensland who supported this project since its beginning. They acknowledge the support of the Department of Civil Engineering at the University of Queensland which provided the experimental facility and the financial support of Australian Research Council (Ref. No. A89331591). The first author was supported by an Australian Postgraduate Award during his Ph.D. thesis.

The authors appreciate the helpful comments of the anonymous reviewers and of the associated technical editor, Professor O. C. Jones.

References

Bin, A. K., 1993, "Gas Entrainment by Plunging Liquid Jets," *Chemical Engineering Science*, Vol. 48, No. 21, pp. 3585-3630.
Bonetto, F., and Lahey, R. T. Jr., 1993, "An Experimental Study on Air Carryunder due to a Plunging Liquid Jet," *International Journal of Multiphase Flow*, Vol. 19, No. 2, pp. 281-294. Discussion: Vol. 20, No. 3, pp. 667-770.

Bonetto, F., Drew, D., and Lahey, R. T. Jr., 1994, "The Analysis of a Plunging Liquid Jet—The Air Entrainment Process," *Chemical Engineering Communication*, Vol. 130, pp. 11-29.
Burley, R., and Jolly, R. P. S., 1984, "Entrainment of Air into Liquids by a High Speed Continuous Solid Surface," *Chemical Engineering Science*, Vol. 39, No. 9, pp. 1357-1372.
Chanson, H., 1995a, "Air Bubble Entrainment in Free-surface Turbulent Flows. Experimental Investigations." Report CH46/95, Dept. of Civil Engineering, University of Queensland, Australia, June, 368 pages.
Chanson, H., 1995b, "Air Entrainment in Two-dimensional Turbulent Shear Flows with Partially Developed Inflow Conditions," *International Journal of Multiphase Flow*, Vol. 21, No. 6, pp. 1107-1121.
Coles, K. A., 1967, *Heavy Weather Sailing*, Adlard Coles, London, UK, 303 pages.
Crank, J., 1956, *The Mathematics of Diffusion*, Oxford University Press, London, UK.
Cummings, P. D., and Chanson, H., 1997, "Air Entrainment in the Developing Flow Region of Plunging Jets. Part 2," *ASME JOURNAL OF FLUIDS ENGINEERING*, published in this issue pp. 603-608.
Ervine, D. A., McKeogh, E. J., and Elsway, E. M., 1980, "Effect of Turbulence Intensity on the rate of Air Entrainment by Plunging Water Jets," *Proceedings of the Institution of Civil Engineers*, Part 2, June, pp. 425-445.
Evans, G. M., 1990, "A Study of a Plunging Jet Bubble Column," Ph.D. thesis, Univ. of Newcastle, Australia.
Fischer, H. B., List, E. J., Koh, R. C. Y., Imberger, J., and Brooks, N. H., 1979, *Mixing in Inland and Coastal Waters*, Academic Press, New York, USA.
Goldring, B. T., Mawer, W. T., and Thomas, N., 1980, "Level Surges in the Circulating Water Downshaft of Large Generating Stations," *Proceedings of 3rd International Conference on Pressure Surges*, BHRA Fluid Eng., F2, Canterbury, U.K., pp. 279-300.
Lezzi, A. M., and Prosperetti, A., 1991, "The Stability of an Air Film in a Liquid Flow," *Journal of Fluid Mechanics*, Vol. 226, pp. 319-347.
Longuet-Higgins, M. S., 1982, "Parametric Solutions for Breaking Waves," *Journal of Fluid Mechanics*, Vol. 121, pp. 403-424.
McKeogh, E. J., 1978, "A Study of Air Entrainment using Plunging Water Jets," Ph.D. thesis, Queen's University of Belfast, UK, 374 pages.
McKeogh, E. J., and Ervine, D. A., 1981, "Air Entrainment rate and Diffusion Pattern of Plunging Liquid Jets," *Chemical Engineering Science*, Vol. 36, pp. 1161-1172.
Michel, J. M., 1984, "Some Features of Water Flows with Ventilated Cavities," *ASME JOURNAL OF FLUIDS ENGINEERING*, Sept., Vol. 106, p. 319.
Sene, K. J., 1988, "Air Entrainment by Plunging Jets," *Chemical Engineering Science*, Vol. 43, No. 10, pp. 2615-2623.
Van de Donk, J., 1981, "Water Aeration with Plunging Jets." Ph.D. thesis, TH Delft, The Netherlands, 168 pages.
Van de Sande, E., 1974, "Air Entrainment by Plunging Water Jets." Ph.D. thesis, TH Delft, The Netherlands, 123 pages.
Van de Sande, E., and Smith, J. M., 1973, "Surface Entrainment of Air by High Velocity Water Jets," *Chemical Engineering Science*, Vol. 28, pp. 1161-1168.